


RESEARCH PAPER



## Myotubularin related protein 7 is essential for the spermatogonial stem cell homeostasis via PI3K/AKT signaling

Dan Zhao<sup>a\*</sup>, Cong Shen <sup>b,c,\*</sup>, Tingting Gao<sup>d\*</sup>, Hong Li<sup>b\*</sup>, Yueshuai Guo<sup>c,e\*</sup>, Feng Li<sup>a,f</sup>, Chenchen Liu<sup>c</sup>, Yuanyuan Liu<sup>b,c</sup>, Xia Chen<sup>g</sup>, Xi Zhang<sup>c</sup>, Yangyang Wu<sup>c</sup>, Yi Yu<sup>b</sup>, Meng Lin<sup>c</sup>, Yan Yuan<sup>h</sup>, Xiaofang Chen<sup>a</sup>, Xiaoyan Huang<sup>c</sup>, Shenmin Yang<sup>b</sup>, Jun Yu<sup>g</sup>, Jun Zhang<sup>c</sup>, and Bo Zheng 

<sup>a</sup>Fourth Affiliated Hospital of Jiangsu University, Zhenjiang, China; <sup>b</sup>Center for Reproduction and Genetics, Suzhou Municipal Hospital, the Affiliated Suzhou Hospital of Nanjing Medical University, Suzhou, China; <sup>c</sup>State Key Laboratory of Reproductive Medicine, Department of Histology and Embryology, Nanjing Medical University, Nanjing, China; <sup>d</sup>Center of Clinical Reproductive Medicine, the Affiliated Changzhou Maternity and Child Health Care Hospital of Nanjing Medical University, Changzhou, China; <sup>e</sup>The Affiliated Wuxi Maternity and Child Health Care Hospital of Nanjing Medical University, Wuxi, China; <sup>f</sup>Reproductive Medicine Center, Northern Jiangsu Province Hospital, Yangzhou, China; <sup>g</sup>Department of Obstetrics and Gynecology, Affiliated Hospital of Jiangsu University, Jiangsu University, Zhenjiang, China; <sup>h</sup>Human Reproductive and Genetic center, Affiliated Hospital of Jiangnan University, Wuxi, China

### ABSTRACT

Myotubularin related protein 7 (MTMR7), a key member of the MTMR family, depicts phosphatase activity and is involved in myogenesis and tumor growth. We have previously identified MTMR7 in the proteomic profile of mouse spermatogonial stem cell (SSC) maturation and differentiation, implying that MTMR7 is associated with neonatal testicular development. In this study, to further explore the distribution and function of MTMR7 in mouse testis, we studied the effect of *Mtmr7* knockdown on neonatal testicular development by testicular and SSC culture methods. Our results revealed that MTMR7 is exclusively located in early germ cells. Deficiency of MTMR7 by morpholino in neonatal testis caused excessive SSC proliferation, which was attributable to the aberrant PI3K/AKT signaling activation. Altogether, our study demonstrates that MTMR7 maintains SSC homeostasis by inhibiting PI3K/AKT signaling activation.

### ARTICLE HISTORY

Received 19 May 2019  
Revised 14 August 2019  
Accepted 21 August 2019

### KEYWORDS

Myotubularin related protein 7 (MTMR7); spermatogonial stem cell (SSC); germ cells; PI3K/AKT signaling

## Introduction


Spermatogonial stem cells (SSCs) belong to undifferentiated germ cells that have the potential to self-renew and differentiate into committed progenitors that maintain the life-long spermatogenesis [1]. Undifferentiated spermatogonia can be subdivided into spermatogonial type A single (As; isolated single cells), A paired (Apr; chains of two cells) and A aligned (Aal; chains of 4–16 cells) [2]. Based on live imaging and mathematical modeling, recent studies have emphasized the roles of As, Apr and Aal spermatogonia to the SSC population [3,4]. Postnatally, SSCs arise from more undifferentiated gonocytes, which are derived from primordial germ cells (PGCs). The transition of gonocytes into SSCs takes place between 0 and 6 d postpartum (dpp) in mice, with the first appearance of SSCs occurring at 3–4 dpp [5]. Similar to other stem cells, SSCs maintain

prolonged tissue homeostasis by continuously self-renewing, proliferating, and differentiating. However, the molecular mechanisms underlying their regulation remain largely unknown [6].

Myotubularin related proteins (MTMRs) are a highly conserved family that includes 15 members, namely Myotubularin 1 and MTMR1 to MTMR14, each possessing distinct functions [7–9]. According to previous studies, MTMR7 displays phosphatase activity that specifically dephosphorylates the D-3 position of phosphatidylinositol 3-phosphate (PI(3)P) and phosphatidylinositol 1,3-bisphosphate (PI(1,3)P2), generating PI and PI(5)P, which are the primary substrates for phosphatidylinositol-3, 4, 5-trisphosphate (PIP3) synthesis [10,11]. PIP3 is a key messenger in PI3K/AKT signaling, which plays a multifunctional role in cellular processes such as cell proliferation, migration, differentiation and apoptosis [12].

**CONTACT** Cong Shen  344128944@qq.com; Shenmin Yang  drim2004@126.com; Jun Yu  yujun9117@126.com; Jun Zhang  zhang\_jun@njmu.edu.cn; Bo Zheng  mansnoopy@163.com

\*These authors contributed equally to this work

 Supplemental data for this article can be accessed here.

© 2019 Informa UK Limited, trading as Taylor & Francis Group

Depletion of MTMR7 reportedly enhances Th17 cell differentiation, accompanied by an increase in AKT phosphorylation [13]. In addition, MTMR7 is known to inhibit AKT-ERK1/2 signaling and proliferation in human colorectal cancer cell lines [14]. Further, Yuan *et al.* recently reported that knocking down MTMR7 promotes myoblast proliferation via AKT signaling [15].

In our previous work, we successfully identified MTMR7 in the proteomic profile of neonatal mouse testis [16]. Bioinformatic analysis in our study suggested that MTMR7 is related to germ cell development. In the present study, we aimed to study the distribution of MTMR7 in neonatal mouse testis, and study the effects of its knock-down *in vitro*. Our research supported that MTMR7 plays a pivotal role in the SSC proliferation via PI3K/AKT signaling.

## Materials and methods

### Animals

Pregnant ICR mice were maintained in a controlled environment under a 12/12-h light/dark cycle at 20–22°C and 50–70% humidity with food and water available *ad libitum*. All mouse experiments were conducted in conformity with the guidelines of the Ethics Committee of Nanjing Medical University.

### Immunofluorescence

Mouse testis tissues and explants were fixed in 4% (*w/v*) paraformaldehyde, embedded in paraffin and sectioned into 5- $\mu$ m thick sections. For immunofluorescence, sections were deparaffinized in xylene and rehydrated in a graded ethanol series. Following antigen retrieval in sodium citrate buffer (pH 6.0) at 100°C for 10 min and blockage of nonspecific sites with 1% BSA (*w/v*), tissues were incubated overnight at 4°C with primary antibodies (Supplementary Table S1). Sections were washed with phosphate-buffered saline-Tween and reacted with Alexa-Fluor secondary antibodies (Thermo Scientific, Waltham, USA) for 1 h at room temperature, and the nucleus was stained with DAPI. Images were acquired using a confocal laser microscope (Zeiss LSM710, Carl

Zeiss, Oberkochen, Germany). For SSCs immunofluorescence, SSCs were cultured in a Millicell EZ slide (Merck Millipore Corporation, Darmstadt, Germany). Cells were fixed in 4% (*w/v*) paraformaldehyde, blocked with 1% BSA (*w/v*) and then reacted overnight at 4°C with primary antibodies (Supplementary Table S1). After subsequent washes, the samples were incubated with Alexa-Fluor secondary antibodies (Thermo Scientific, Waltham, USA). All samples were examined under a confocal laser microscope (Zeiss LSM710, Carl Zeiss, Oberkochen, Germany).

### Western blot analysis

Western blot was carried out as described previously with minor modifications [17]. In short, tissue lysates were separated by electrophoresis on polyacrylamide and electrotransferred to polyvinylidene difluoride membranes (Bio-Rad, Hercules, USA). The membranes were then blocked with 5% (*w/v*) non-fat dried milk and incubated overnight at 4°C with the indicated primary antibodies (Supplementary Table S1). Blots were then washed with phosphate-buffered saline-Tween and incubated at room temperature for 1 h with horseradish peroxidase-conjugated secondary antibodies (Thermo Scientific, Waltham, USA). The immunocomplexes signals were visualized by enhanced chemiluminescent (Thermo Scientific, Waltham, USA). Image Pro Plus analysis of the resultant band was subsequently performed.

### TUNEL assay

Apoptotic cells were assayed using TUNEL BrightRed Apoptosis Detection Kit (Vazyme, Nanjing, China), according to the manufacturer's instructions. Briefly, sections were deparaffinized and rehydrated in a graded ethanol series and incubated with 20  $\mu$ g/ml proteinase K for 10 min. The sections were then treated with equilibration buffer for 30 min at room temperature, followed by BrightRed Labeling Buffer for 60 min at 37°C. After washing with phosphate-buffered saline-Tween for 3 times, samples were stained with DAPI. Images were captured using a confocal laser microscope (Zeiss LSM710, Carl Zeiss, Oberkochen, Germany).

### Neonatal testis culture

Testes from 3.5-d mice were decapsulated and gently separated into several 2- to 4-mm-diameter pieces. The tissue explants were placed on stands made of 1.5% (w/v) agarose gel stands (10 × 10 × 5 mm [3] in size and placed in 24-well plates), and cultured as previously described [18]. The amount of medium was half to four-fifth of the height of the agarose gel. Totally 3–5 testes explants were placed on the medium/air interface of each stand and incubated in 5% carbon dioxide in air and maintained at 34°C. Medium was replaced every 2 d. The culture media consisted of  $\alpha$ -minimum essential medium ( $\alpha$ -MEM), with 10% KnockOut serum replacement (KSR), 1% non-essential amino acid solution (NEAA), 0.1%  $\beta$ -mercaptoethanol, as well as 1% penicillin-streptomycin solution. MTMR7-translation-blocking-vivo-Mo (oligo Sequence: CGTG CGGATGTGCTCCAT) and its negative control (oligo Sequence: CCTCTTACCTCAGTTA CAATTTATA) were obtained from Gene Tools (Philomath, Oregon, USA).

### RNA extraction and quantitative PCR

Total RNA was isolated using the RNeasy Plus Micro Kit (Qiagen, Duesseldorf, Germany), according to the manufacturer's instructions. cDNA was reverse transcribed and then subjected to real-time quantitative PCR assay in an ABI 7300 real-time PCR system (Applied Biosystems, Foster City, CA, USA). The primers used are listed in Supplementary Table S2. Gene expression was calculated using  $2^{-\Delta\Delta Ct}$  method, with 18s rRNA as an internal control.

### SSC culture

Long-term culture of mouse SSCs was performed according to our previous described using StemPro-34 SFM [19]. Shortly, testes from 2-d neonatal mice were digested with 1 mg/ml collagenase (type IV; Sigma-Aldrich, St. Louis, MO, USA) for 15 min at 37°C, followed by 0.25% trypsin (Thermo Scientific, Waltham, USA) with 1.4 mg/ml DNase (Sigma-Aldrich, St. Louis, MO, USA) for 10 min at 34°C.

Dispersed testicular cells were cultured on a 0.2% (w/v) gelatin-coated plate overnight. Floating cells were passaged to secondary plates. These cells were then passaged two or three times before they were transferred to a medium containing feeder cells. The cells were cultured in 5% carbon dioxide in air and maintained at 37°C. SSCs were cultured for 5–6 d, either with 10  $\mu$ M MTMR7 or Ctr morpholinos.

### Statistical analysis

Experiments were repeated at least three times. Quantitative results are presented as mean  $\pm$  standard deviation (SD). The statistical significance of the data was determined by either an unpaired Student's t-test or one-way ANOVA followed by the post-hoc tukey's test with \*  $p < 0.05$ ; \*\* $p < 0.01$ ; \*\*\* $p < 0.001$ .

## Results

### MTMR7 expression pattern during spermatogenesis in mice

We performed immunostaining to analyze the distribution of MTMR7 at 3.5-d, 2-wk, 4-wk, and adult mouse testis during the first wave of spermatogenesis. As promyelocytic leukemia zinc finger (PLZF) has a well-defined role in SSC maintenance, herein, it was used as a marker of undifferentiated SSCs [16]. We observed that MTMR7 was exclusively expressed in the cytoplasm of SSCs of 3.5-d testis (Figure 1(a)), as well as in cultured SSCs (Figure 1(b)). The above expression data suggest that MTMR7 is associated with the development of neonatal testes and SSCs.

### MTMR7 knockdown and SSC development

To investigate the function of MTMR7 in neonatal testis, we used morpholino (Mo) oligo to knock-down MTMR7 in the cultured testis explants (Figure 2(a)). Western blot analysis showed 58% silencing efficiency of MTMR7 by Mo *in vitro* (Figure 2(b,c)).

The cultured testis explants incubated with Mo for 4 d were assayed by immunostaining, and the results revealed a significant elevation of LIN28-labeled SSCs [20] (Figure 3(a,b)) and

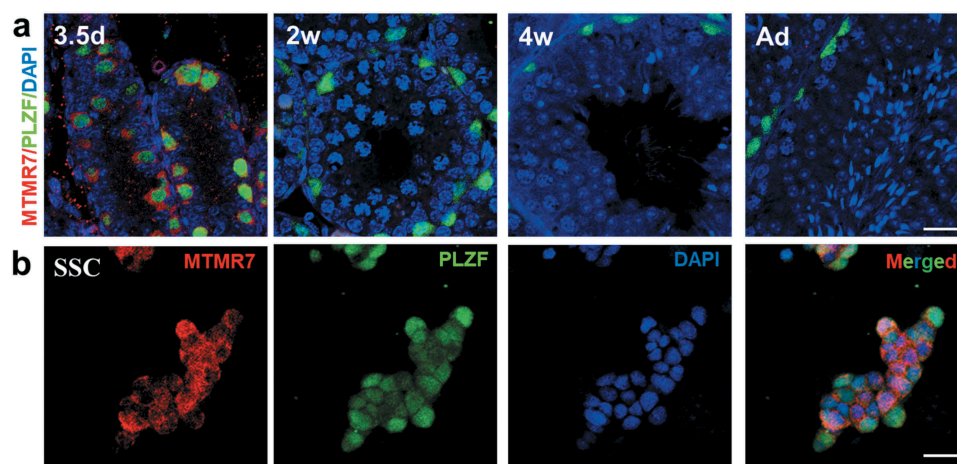


**Figure 1.** Expression of MTMR7 in testis and SSC. (a) Co-immunostaining of MTMR7 and PLZF (undifferentiated spermatogonia marker) at 3.5-d, 2-wk, 4-wk and adult mouse testis. (b) Co-immunostaining of MTMR7 and PLZF in SSC. Scale bar: 20  $\mu\text{m}$ .

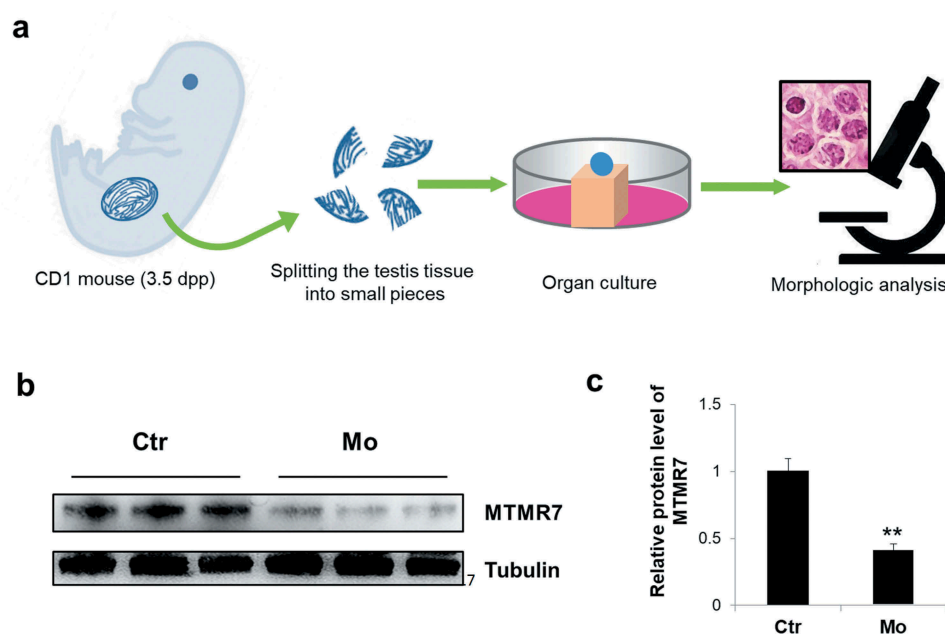


**Figure 2.** Establishment of neonatal testis culture platform. (a) Schematic representation of neonatal testis culture. Neonatal testis was cut into pieces and placed on the medium/air interface of agarose gel stand. The fragments were cultured for 4 d either with 20  $\mu\text{M}$  Mo or its Ctr. (b,c) Western blot analysis showed high knockdown efficiency of MTMR7 by Mo. (\*\* $p < 0.01$ , Student's t-test, sample number = 3).

DDX4-labeled germ cells [21] in the Mo group (Figure 3(c,d)). LIN28- and DDX4-positive cells showed 1.56-fold (from  $78.0 \pm 9.3/10^5\mu\text{m}^2$  to  $121.4 \pm 14.1/10^5\mu\text{m}^2$ ) and 1.41-fold (from  $120.8 \pm 11.7/10^5\mu\text{m}^2$  to  $171 \pm 15.9/10^5\mu\text{m}^2$ ) increase in Mo testes, respectively, compared with the negative control (Ctr) (Figure 3(b,d)). In agreement with this finding, we observed 2.03-fold (from  $28.1 \pm 6.2/10^5\mu\text{m}^2$  to  $57.2 \pm 11.3/10^5\mu\text{m}^2$ ) and 2.25-fold (from

$10.9 \pm 3.9/10^5\mu\text{m}^2$  to  $24.5 \pm 7.6/10^5\mu\text{m}^2$ ) increase of proliferative marker of KI67 [22]- and PH3 [23]-labeled SSC proliferation (Figure 3(e-h)) in Mo testes, while the apoptotic signals remained unchanged between the two groups (Supplementary Figure S1). These data indicate that MTMR7 is pivotal for the regulation of SSC proliferation. To further explore the consequence of the excessive proliferation of SSCs observed in Mo testes, testis explants



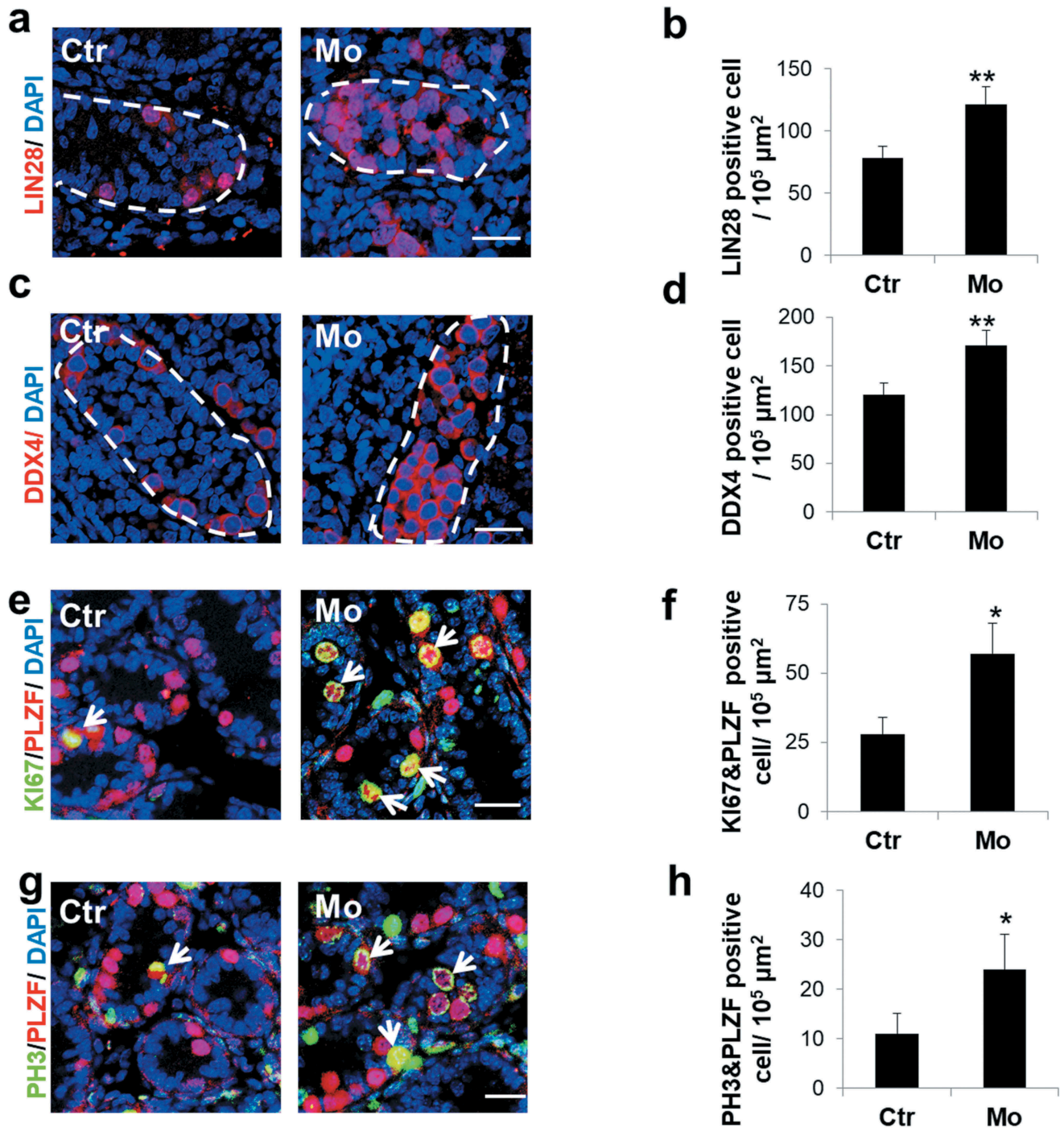


**Figure 3.** MTMR7 is required for germ cell development. (a,b) Representative images of LIN28 (undifferentiated spermatogonia marker) immunostaining in Ctr and Mo testes. (c,d) Representative images of DDX4 (germ cell marker) immunostaining in Ctr and Mo testes. (e,f) Co-immunostaining of KI67 (cellular proliferation marker) and PLZF in Ctr and Mo testes. (g,h) Co-immunostaining of PH3 (cellular proliferation marker) and PLZF in Ctr and Mo testes. Dotted lines indicate seminiferous tubule. White arrows indicate proliferating SSC. (\* $p < 0.05$ , \*\* $p < 0.01$ , Student's t-test, sample number = 6). Scale bar: 20  $\mu\text{m}$ .

from 3.5-d were cultured for 11 d, which corresponded to the spermatocyte stage. In contrast to Ctr, the number of spermatocytes (labeled by  $\gamma\text{H2AX}$  [24]) in Mo testes displayed

markedly decreased (from  $159.6 \pm 24.8/10^5 \mu\text{m}^2$  to  $20.6 \pm 6.2/10^5 \mu\text{m}^2$ ) (Supplementary Figure S2), revealing that MTMR7-deficient SSCs lose the function to enter meiosis.

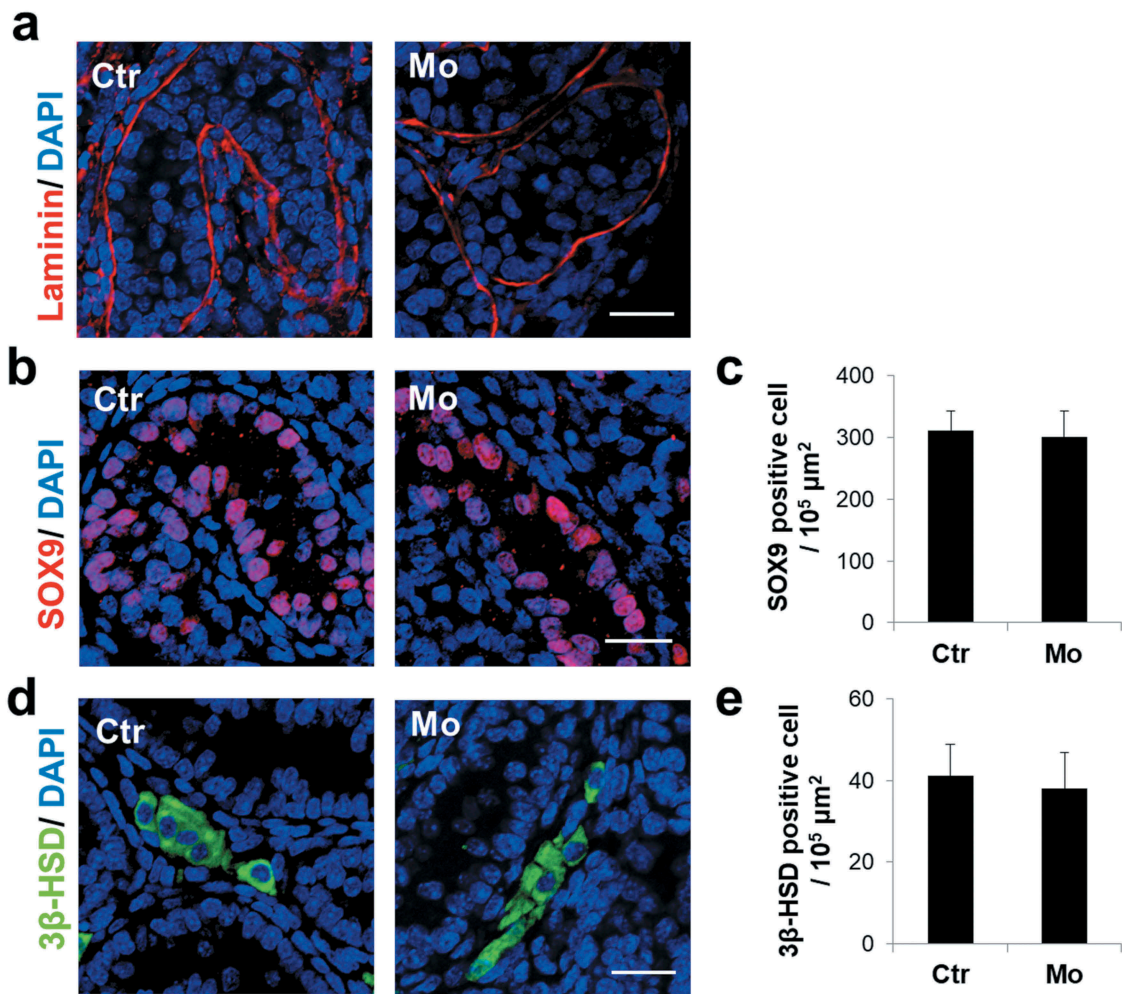


**Figure 4.** MTMR7 knockdown does not disrupt the integrity of seminiferous tubules and somatic cells. (a) Representative images of Laminin immunostaining in Ctr and Mo testes. (b,c) Representative images of SOX9 (Sertoli marker) immunostaining in Ctr and Mo testes. (d,e) Representative images of 3β-HSD (Leydig marker) immunostaining in Ctr and Mo testes. (Student's t-test, sample number = 6). Scale bar: 20 μm.

#### **Integrity of seminiferous tubules and somatic cells after MTMR7 knockdown**

To assess the integrity of seminiferous tubules after MTMR7 knockdown, we labeled the basal laminae of testes by laminin [25], and the results revealed that the seminiferous tubules appeared intact in the Mo group (Figure 4(a)). Moreover, we also performed immunostaining of Sertoli and Leydig cells using SOX9 [26] and 3β-HSD [27], respectively, and the results implied that the number of Sertoli and Leydig cells did not appear to differ between the two groups (Figure 4(b-e)).

#### **Depletion of MTMR7 triggers PI3K/AKT signaling, along with cell cycle progression**

Previous studies have demonstrated that knockdown of MTMR7 promotes cell proliferation via AKT signaling [15]. The AKT signaling cascade is originally activated by the production of PIP3, which serves as docking phospholipids to subsequently induce phosphorylation of AKT at Thr308 and Ser473 sites [12]. Here, PIP3 and phosphorylated AKT levels were measured by ELISA and western blot, respectively. And the results exhibited that AKT signaling was dramatically activated in the Mo group, in comparison to Ctr

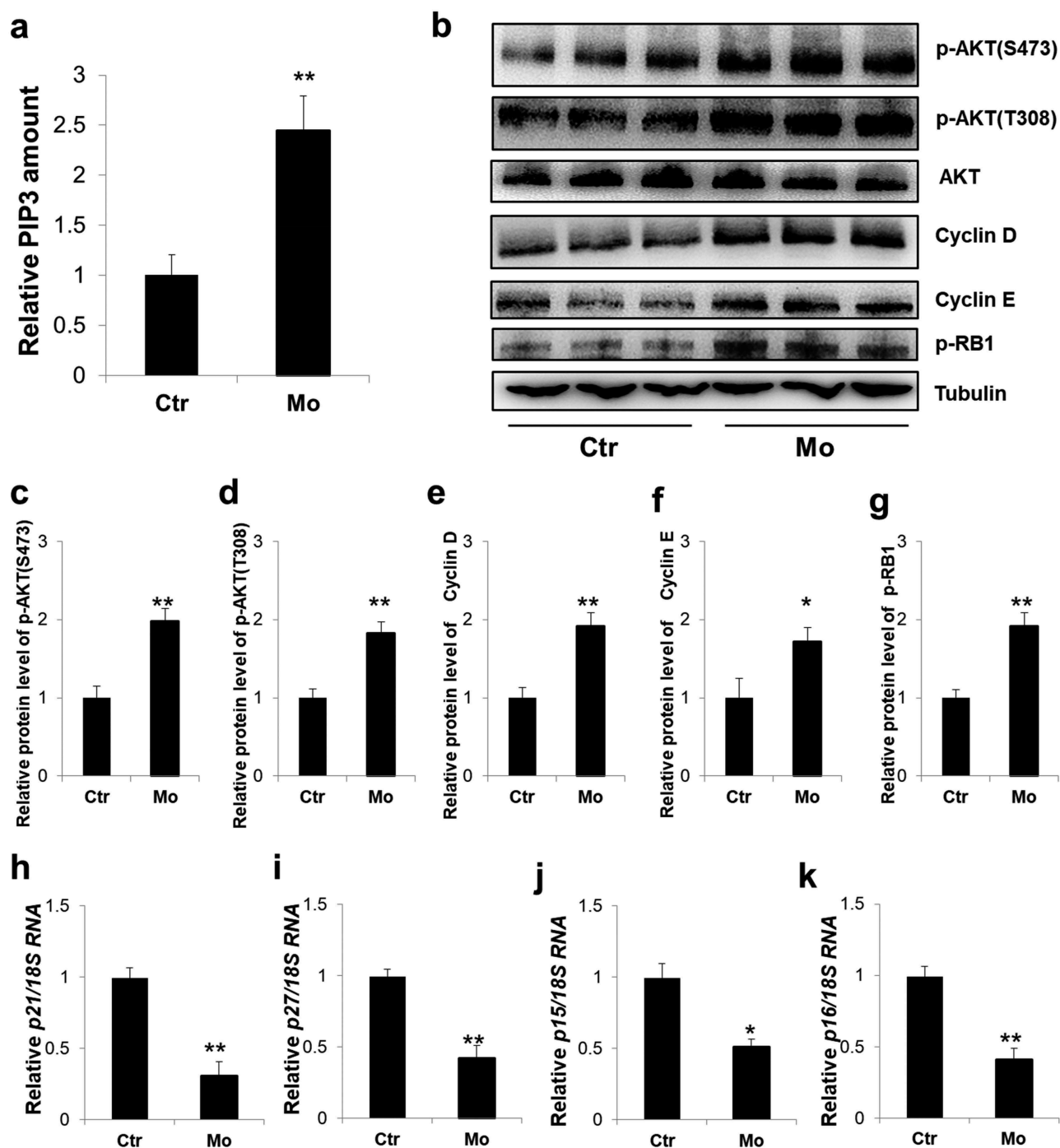


**Figure 5.** Aberrant activation of PI3K/AKT signaling in MTMR7-deficient testes. (a) ELISA assay of the PIP3 level in Ctrl and Mo testes. (b) Western blot analysis of the expression levels of p-AKT(S473), p-AKT(T308), total AKT, Cyclin D, Cyclin E and p-RB1 in Ctrl and Mo testes. (c-g) Quantification of (b). Real-time PCR analysis of the expression levels of *p21* (h), *p27* (i), *p15* (j) and *p16* (k) in Ctrl and Mo testes. (\* $p < 0.05$ , \*\* $p < 0.01$ , Student's t-test. For (b-g) sample number = 3; for (h-k), sample number = 6).

(from  $1.0 \pm 0.2$  to  $2.45 \pm 0.34$  for PIP3; from  $1.0 \pm 0.15$  to  $1.9 \pm 0.16$  for p-AKT(S473); from  $1.0 \pm 0.11$  to  $1.8 \pm 0.14$  for p-AKT(T308)) (Figure 5(a-g)). Cell cycle is tightly regulated by Cyclin-dependent kinases (CDKs)

[28] and their opponents, Cyclin-dependent kinase inhibitor proteins (CDKIs) [29]. In line with the excessive cellular proliferation found in Mo testes, Cyclin-dependent kinase inhibitor proteins (CDKIs), p21,



p27, p15 and p16 were apparently depressed (from  $1.0 \pm 0.07$  to  $0.31 \pm 0.09$  for p27; from  $1.0 \pm 0.05$  to  $0.42 \pm 0.09$  for p15; from  $1.0 \pm 0.1$  to  $0.51 \pm 0.05$  for p16) (Figure 5(h-k)), whereas cell cycle positive regulators, Cyclin D, Cyclin E, as well as phosphorylated retinoblastoma tumor suppressor protein (p-RB1) displayed obvious elevation (from  $1.0 \pm 0.13$  to  $1.92 \pm 0.17$  for Cyclin D; from  $1.0 \pm 0.25$  to  $1.72 \pm 0.18$  for Cyclin E; from  $1.0 \pm 0.11$  to  $1.93 \pm 0.17$  for p-RB1) in Mo testes (Figure 5(b-g)).

### **Inhibition of PI3K/AKT signaling can partly rescue the altered phenotypes in MTMR7-deficient testes**

To verify whether aberrant activation of the PI3K/AKT pathway was a vital contributor to the excessive proliferation of SSCs observed in this study, we treated cultured testicular cells with the PI3K/AKT pathway inhibitor, LY294002 (10  $\mu$ M) [30]. Western blot results indicated that LY294002 inhibited the AKT pathway with a high efficiency (Figure 6(a-c)). Immunostaining results revealed that the number of germ cells labeled by LIN28 and DDX4 in the LY294002-treated Mo group showed a 19.2% (from  $130.4 \pm 9.3/10^5 \mu\text{m}^2$  to  $105.3 \pm 3.2/10^5 \mu\text{m}^2$ ) and 23.5% (from  $169.5 \pm 6.6/10^5 \mu\text{m}^2$  to  $129.6 \pm 4.3/10^5 \mu\text{m}^2$ ) decline, respectively, compared with the Mo group (Figure 6(d-g)). Accordingly, proliferating SSC labeled by KI67 and PH3 in the LY294002-treated Mo group displayed a 32.5% (from  $45.5 \pm 3.2/10^5 \mu\text{m}^2$  to  $30.7 \pm 4.1/10^5 \mu\text{m}^2$ ) and 35.2% (from  $31.8 \pm 2.0/10^5 \mu\text{m}^2$  to  $20.6 \pm 1.2/10^5 \mu\text{m}^2$ ) reduce, respectively, in comparison to the Mo group (Figure 6(h-k)). In line with the above findings, the amount of Cyclins, p-RB1 and CDKIs in LY294002-treated Mo group exhibited reversed expressions, compared with the Mo group (Supplementary Figure S3(a-h)).

### **Deficiency of MTMR7 promotes SSC proliferation in vitro**

To further confirm whether MTMR7 knockdown was a direct contributor of the observed SSC proliferation, we incubated SSC culture with Mo. As shown in Figure 7(a-d), the proliferation signals in the Mo treatment group were apparently increased, compared

with Ctr. Also, the SSC colony size in the Mo group was obviously larger than that in the Ctr group (from  $2939 \pm 430 \mu\text{m}^2$  to  $4841 \pm 170 \mu\text{m}^2$ ) (Figure 7(a,c,e)). Furthermore, we treated cultured SSCs with 10  $\mu$ M LY294002 in Mo group, immunostaining results showed that the proportion of proliferating SSCs labeled by PH3 and KI67 in the LY294002-treated Mo group depicted 45% (from  $38.9 \pm 4.5\%$  to  $21.6 \pm 1.9\%$ ) and 47.5% (from  $62 \pm 7.4\%$  to  $32.5 \pm 4.6\%$ ) drop, respectively, in comparison to Mo (Figure 7(a-d)). As expected, Mo group evinced measurable decreased amounts of CDKIs, whereas treatment of LY294002 in Mo showed reverse expression (Figure 7(f-i)). To further show morpholino specificity, cultured SSCs were successfully transfected with pcDNA3.0-MTMR7 overexpression vector (Supplementary Figure S4(a,b)). Consistent with LY294002 rescuing SSC proliferation (Figure 7(a-e)), MTMR7-treated Mo group exerted antiproliferative effects as well (Supplementary Figure S4(c-f)). Altogether, the excessive cell proliferation observed in MTMR7-deficient SSCs (Figure 7(a-i) and Supplementary Figure S4(a-f)) was highly consistent with findings pertinent to MTMR7-deficient testes (Figure 3(a-h)).

## **Discussion**

Our study is the first to address the question of the distribution and function of MTMR7 in mammalian SSCs and testis. We found that MTMR7 was exclusively located in SSCs. Pioneering study by Sato *et al.* first obtained functional sperm in cultured neonatal mouse testis [18], we as well as other researchers have widely used this culture method as a platform to gain mechanistic understanding of spermatogenesis [31–34]. As for SSC culture, it is also a reliable model to explore the development of SSCs and intricate mechanisms of spermatogenesis [19,35,36]. By neonatal testis and SSC culture, we noted that knockdown of MTMR7 by Mo caused excessive SSC proliferation and PI3K/AKT pathway activation. Moreover, treatment with the PI3K/AKT pathway inhibitor, LY294002, could partly rescue the altered phenotypes. Our results demonstrate that MTMR7 regulates SSC development, mainly via influencing PI3K/AKT signaling.

SSCs have unique properties to self-renew and support spermatogenesis throughout their lifespan,



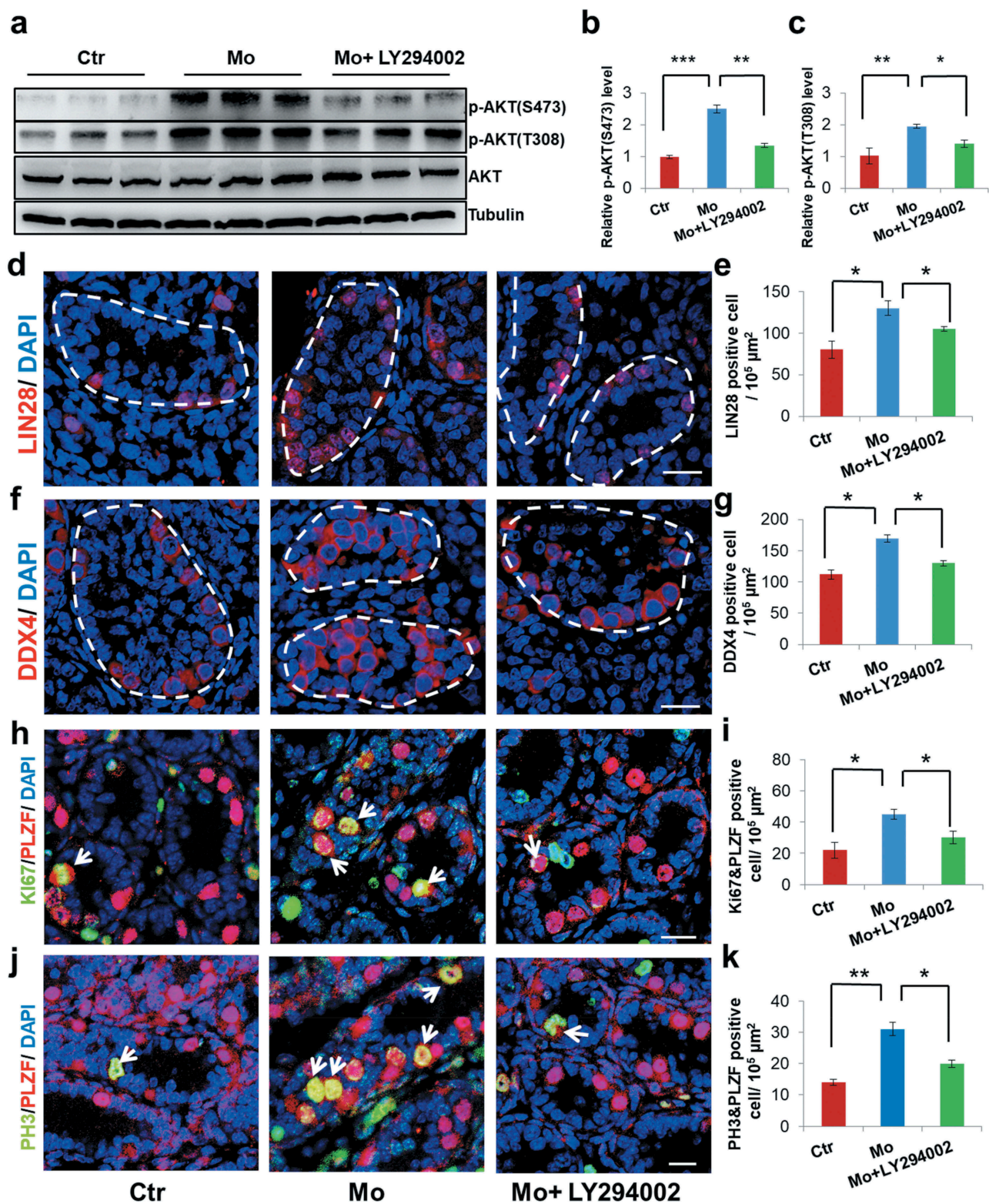


**Figure 6.** PI3K inhibitor, LY294002, can partly rescue the altered phenotypes. (a,b,c) Western blot analysis showed p-AKT(S473), p-AKT(T308) and total AKT levels in Ctrl, Mo and Mo+ LY294002 testes. (d,e) Representative images of LIN28 immunostaining in Ctrl, Mo and Mo+ LY294002 testes. (f,g) Representative images of DDX4 immunostaining in Ctrl, Mo and Mo+ LY294002 testes. (h,i) Co-immunostaining of Ki67 and PLZF in Ctrl, Mo and Mo+ LY294002 testes. (j,k) Co-immunostaining of PH3 and PLZF in Ctrl, Mo and Mo+ LY294002 testes. Dotted lines indicate seminiferous tubule. White arrows indicate proliferating SSC. (\* $p < 0.05$ , \*\* $p < 0.01$ , \*\*\* $p < 0.001$ , one-way ANOVA. For (a-c), sample number = 3; for (d-k), sample number = 6). Scale bar: 20  $\mu\text{m}$ .

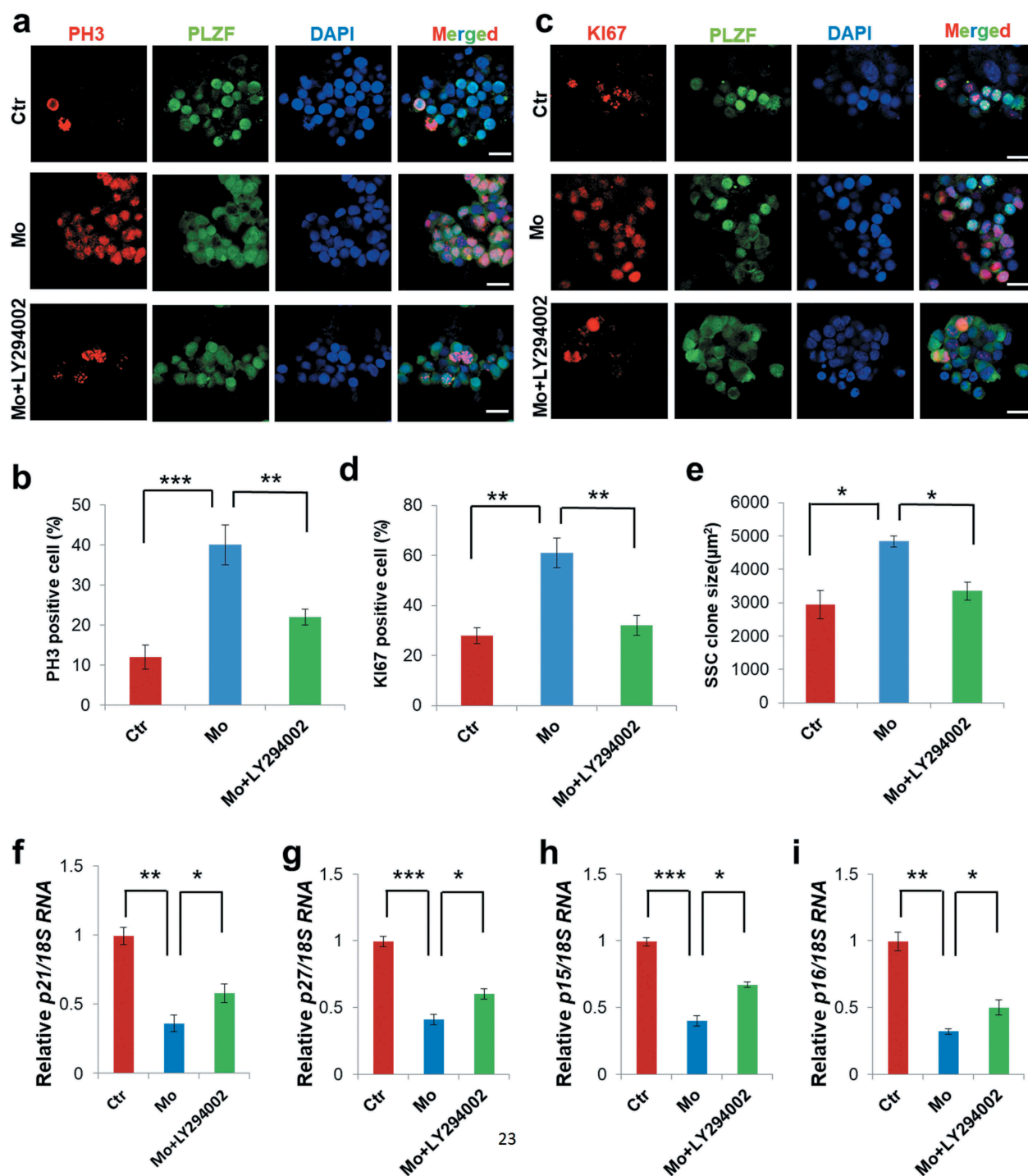


**Figure 7.** Influence of MTMR7 knockdown on SSC culture. (a,b) Co-immunostaining of PH3 and PLZF in Ctr, Mo and Mo+ LY294002 SSCs. (c,d) Co-immunostaining of KI67 and PLZF immunostaining in Ctr, Mo and Mo+ LY294002 SSCs. (e) Quantification of SSC clone. Real-time PCR analysis of the expression levels of *p21* (f), *p27* (g), *p15* (h) and *p16* (i) in Ctr, Mo and Mo+ LY294002 SSCs. (\* $p < 0.05$ , \*\* $p < 0.01$ , \*\*\* $p < 0.001$ , one-way ANOVA, sample number = 4). Scale bar: 20  $\mu\text{m}$ .

and the pool of SSCs needs to be strictly maintained with a dynamic balance [37]. More self-renewal than differentiation could diminish the seminiferous

epithelium to only stem cells and a tumor might form. If differentiation prevailed, stem cells would deplete themselves, inducing seminiferous lumens

with only the supporting Sertoli cells. Cumulating evidence has demonstrated that GDNF, Lin28a, Dmrt1, B7-H3 and miR-100 promote SSC proliferation [38–42], while miR-204 and Mir146a suppress SSC proliferation [43,44]. During cell cycle, Cyclin-dependent kinases (CDKs) and their regulatory binding partners, cyclins, comprise the central machinery and promote cell cycle progression. Alternatively, Cyclin-dependent kinase inhibitor proteins (CDKIs) inhibit CDKs activity, thus inducing cell cycle arrest [45]. There are two classes of CDKIs, namely inhibitors of CDK4 (INK4) and kinase inhibitors proteins (KIPs), respectively. INK4 members, p15, p16, p18 and p19, can specifically bind CDK4/6 and inhibit their link with Cyclin D. Whereas p21, p27 as well as p57 from KIPs are recognized as inhibitors of Cyclin E-CDK2 complex [46]. During G1 to S phase transition, the retinoblastoma tumor suppressor protein (RB1) is phosphorylated by Cyclin D-CDK4/6 followed by Cyclin

E-CDK2, which in turn releasing transcriptional factor, E2F, and allowing E2F-mediated S phase gene transcription [47,48]. In our study, depletion of MTMR7 led to PI3K/AKT activation, followed by the depression of CDKIs (p15, p16, p21 and p27) and up-regulation of CDKs (Cyclin D and Cyclin E), and finally causing RB1 hyperphosphorylation (Figure 8). In all, we extrapolated that MTMR7 could negatively regulate cell cycle of SSCs in G1-S phase transition.

PI3Ks form a family of kinases expressed in virtually all mammalian cells with essential roles in cell cycle progression, survival, migration, and cell growth [49]. AKT is the most studied and universally activated molecule downstream of PI3Ks [50]. Previous studies have proved that AKT activity is involved in cell proliferation, metabolism, survival, and motility by the phosphorylation of a myriad of downstream effector molecules [51]. Early researchers have confirmed that the AKT pathway is associated with the

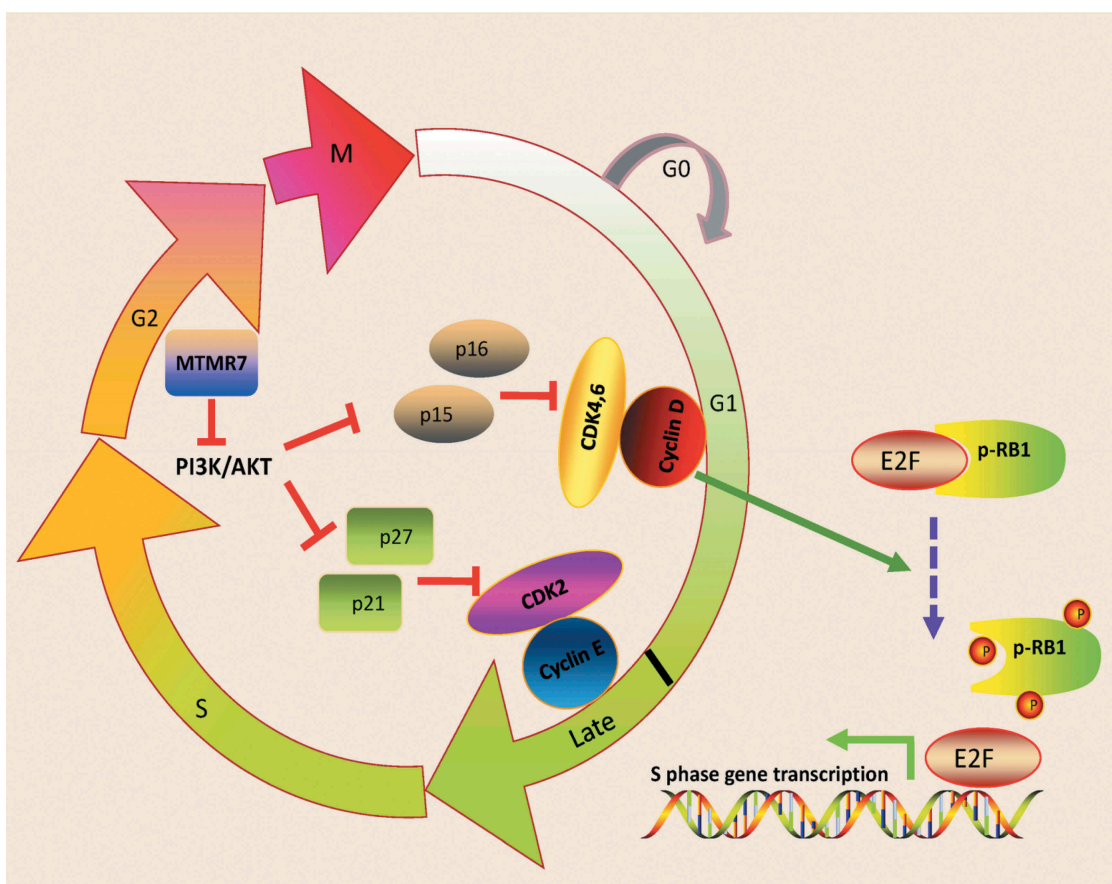


**Figure 8.** Schematic illustration of MTMR7 work model. MTMR7 acts as a negative regulator of cell cycle via depressing PI3K/AKT signaling. Knockdown of MTMR7 leads to PI3K/AKT activation, followed by the inactivated of CDKIs (p21, p27, p15 and p16). Then, cyclin D-CDK4,6 and cyclin E-CDK2 complex phosphorylate RB1, thus, contributing to E2F transcriptional activity and promoting G1-S phase transition.



growth of SSCs. For instance, Ma *et al.* suggested that Lin28a activates the AKT signaling pathway to promote the proliferation and maintain the self-renewal of dairy goat SSC [39]. Feng *et al.* reported that stem cell factor (SCF)/C-kit promotes the proliferation of type A spermatogonia by recruiting PI3K/AKT/p70 S6 kinase/cyclin D [52]. Moreover, Liu *et al.* indicated that Setdb1 regulates the AKT pathway to inhibit SSC apoptosis [53]. Consistent with these findings, our present study reports excessive SSC proliferation, in association with aberrant activation of the AKT pathway in MTMR7-deficient neonatal testes and SSCs. Moreover, treatment with an AKT pathway inhibitor resulted in an apparent reverse of phenotypes in neonatal testis culture and SSC culture. Based on these data, we conclude that the PI3K/AKT pathway is one of the crucial targets of MTMR7 and that it plays important roles in neonatal testicular and SSC development in mice.

In summary, we identified a novel factor, MTMR7, that could negatively regulate the proliferation of mouse SSCs through PI3K/AKT pathway. These findings will help to increase our understanding of the self-renewal and differentiation of SSCs.

### Disclosure statement

No potential conflict of interest was reported by the authors.

### Funding

This work was supported by the Suzhou Key Medical Center (SZZX201505), Jiangsu Provincial Medical Innovation Team (CXTDB2017013), Suzhou Introduced Project of Clinical Medical Expert Team (SZYJTD201708), Suzhou Key Laboratory of male reproduction research (SZS201718), Suzhou Science and Technology Development Project (SYS201566), Clinical Medical Foundation of Chinese Medical Association (18010330762), Open Fund of State Key Laboratory of Reproductive Medicine of Nanjing Medical University (SKLRM-KA201704), Basic Program of Nanjing Medical University (2017NJMU163), Natural Science Foundation of Jiangsu Province (BK20160177 and BK20170562), the Science and Technology Project of Changzhou (CJ20180040), Maternity and Child Health Foundation of Jiangsu Province (F201865), National Natural Science Foundation of China (31701298, 81601338), National Science Foundation of the Jiangsu Higher Education Institutions of China (16KJB310006) and Key Research

Foundation of Zhenjiang Social Development (SH2016028, SH2017013 and SH2018065)..

### ORCID

Cong Shen  <http://orcid.org/0000-0002-9982-176X>

Bo Zheng  <http://orcid.org/0000-0002-1496-0753>

### References

- [1] Hermann BP, Phillips BT, Orwig KE. The elusive spermatogonial stem cell marker? *Biol Reprod.* 2011;85:221–223.
- [2] Phillips BT, Gassei K, Orwig KE. Spermatogonial stem cell regulation and spermatogenesis. *Philos Trans R Soc Lond B Biol Sci.* 2010;365:1663–1678.
- [3] Hara K, Nakagawa T, Enomoto H, *et al.* Mouse spermatogenic stem cells continually interconvert between equipotent singly isolated and syncytial states. *Cell Stem Cell.* 2014;14:658–672.
- [4] Nakagawa T, Sharma M, Nabeshima Y, *et al.* Functional hierarchy and reversibility within the murine spermatogenic stem cell compartment. *Science.* 2010;328:62–67.
- [5] McLean DJ, Friel PJ, Johnston DS, *et al.* Characterization of spermatogonial stem cell maturation and differentiation in neonatal mice. *Biol Reprod.* 2003;69:2085–2091.
- [6] de Rooij DG, Russell LD. All you wanted to know about spermatogonia but were afraid to ask. *J Androl.* 2000;21:776–798.
- [7] Robinson FL, Dixon JE. Myotubularin phosphatases: policing 3-phosphoinositides. *Trends Cell Biol.* 2006;16:403–412.
- [8] Laporte J, Blondeau F, Buj-Bello A, *et al.* The myotubularin family: from genetic disease to phosphoinositide metabolism. *Trends Genet.* 2001;17:221–228.
- [9] Maehama T, Taylor GS, Dixon JE. PTEN and myotubularin: novel phosphoinositide phosphatases. *Annu Rev Biochem.* 2001;70:247–279.
- [10] Kim SA, Taylor GS, Torgersen KM, *et al.* Myotubularin and MTMR2, phosphatidylinositol 3-phosphatases mutated in myotubular myopathy and type 4B charcot-marie-tooth disease. *J Biol Chem.* 2002;277:4526–4531.
- [11] Mochizuki Y, Majerus PW. Characterization of myotubularin-related protein 7 and its binding partner, myotubularin-related protein 9. *Proc Natl Acad Sci U S A.* 2003;100:9768–9773.
- [12] Manning BD, Cantley LC. AKT/PKB signaling: navigating downstream. *Cell.* 2007;129:1261–1274.
- [13] Guo L, Martens C, Bruno D, *et al.* Lipid phosphatases identified by screening a mouse phosphatase shRNA library regulate T-cell differentiation and protein



- kinase B AKT signaling. *Proc Natl Acad Sci U S A*. 2013;110:E1849–56.
- [14] Weidner P, Sohn M, Gutting T, et al. Myotubularin-related protein 7 inhibits insulin signaling in colorectal cancer. *Oncotarget*. 2016;7:50490–50506.
- [15] Yuan Z, Chen Y, Zhang X, et al. Silencing myotubularin related protein 7 enhances proliferation and early differentiation of C2C12 myoblast. *Biochem Biophys Res Commun*. 2017;484:592–597.
- [16] Zheng B, Zhou Q, Guo Y, et al. Establishment of a proteomic profile associated with gonocyte and spermatogonial stem cell maturation and differentiation in neonatal mice. *Proteomics*. 2014;14:274–285.
- [17] Kang Y, Zheng B, Shen B, et al. CRISPR/Cas9-mediated Dax1 knockout in the monkey recapitulates human AHC-HH. *Hum Mol Genet*. 2015;24:7255–7264.
- [18] Sato T, Katagiri K, Gohbara A, et al. In vitro production of functional sperm in cultured neonatal mouse testes. *Nature*. 2011;471:504–507.
- [19] Zhou Q, Guo Y, Zheng B, et al. Establishment of a proteome profile and identification of molecular markers for mouse spermatogonial stem cells. *J Cell Mol Med*. 2015;19:521–534.
- [20] Chakraborty P, Buaas FW, Sharma M, et al. LIN28A marks the spermatogonial progenitor population and regulates its cyclic expansion. *Stem Cells*. 2014;32:860–873.
- [21] Kuramochi-Miyagawa S, Watanabe T, Gotoh K, et al. MVH in piRNA processing and gene silencing of retrotransposons. *Genes Dev*. 2010;24:887–892.
- [22] Gerdes J, Lemke H, Baisch H, et al. Cell cycle analysis of a cell proliferation-associated human nuclear antigen defined by the monoclonal antibody Ki-67. *J Immunol*. 1984;133:1710–1715.
- [23] Nowak M, Svensson MA, Carlsson J, et al. Prognostic significance of phospho-histone H3 in prostate carcinoma. *World J Urol*. 2014;32:703–707.
- [24] Hamer G, Roepers-Gajadien HL, van Duyn-Goedhart A, et al. DNA double-strand breaks and gamma-H2AX signaling in the testis. *Biol Reprod*. 2003;68:628–634.
- [25] Zheng QS, Wang XN, Wen Q, et al. Wt1 deficiency causes undifferentiated spermatogonia accumulation and meiotic progression disruption in neonatal mice. *Reproduction*. 2014;147:45–52.
- [26] Symon A, Harley V. SOX9: A genomic view of tissue specific expression and action. *Int J Biochem Cell Biol*. 2017;87:18–22.
- [27] Zheng D, Zhao Y, Shen Y, et al. Orexin A-mediated stimulation of 3beta-HSD expression and testosterone production through MAPK signaling pathways in primary rat leydig cells. *J Endocrinol Invest*. 2014;37:285–292.
- [28] Malumbres M, Barbacid M. Cell cycle, CDKs and cancer: a changing paradigm. *Nat Rev Cancer*. 2009;9:153–166.
- [29] Besson A, Dowdy SF, Roberts JM. CDK inhibitors: cell cycle regulators and beyond. *Dev Cell*. 2008;14:159–169.
- [30] Zheng B, Geng L, Zeng L, et al. AKT2 contributes to increase ovarian cancer cell migration and invasion through the AKT2-PKM2-STAT3/NF-kappaB axis. *Cell Signal*. 2018;45:122–131.
- [31] Zheng B, Yu J, Guo Y, et al. Cellular nucleic acid-binding protein is vital to testis development and spermatogenesis in mice. *Reproduction*. 2018;156:59–69.
- [32] Shen C, Yu J, Zhang X, et al. Strawberry Notch 1 (SBNO1) promotes proliferation of spermatogonial stem cells via the noncanonical Wnt pathway in mice. *Asian J Androl*. 2019;21:345–350.
- [33] Shen C, Zhang K, Yu J, et al. Stromal interaction molecule 1 is required for neonatal testicular development in mice. *Biochem Biophys Res Commun*. 2018;504:909–915.
- [34] Chen M, Wang X, Wang Y, et al. Wt1 is involved in leydig cell steroid hormone biosynthesis by regulating paracrine factor expression in mice. *Biol Reprod*. 2014;90:71.
- [35] Kanatsu-Shinohara M, Tanaka T, Ogonuki N, et al. Myc/Mycn-mediated glycolysis enhances mouse spermatogonial stem cell self-renewal. *Genes Dev*. 2016;30:2637–2648.
- [36] Hesel AR, Yang QE, Oatley MJ, et al. ID4 levels dictate the stem cell state in mouse spermatogonia. *Development*. 2017;144:624–634.
- [37] Lee J, Kanatsu-Shinohara M, Morimoto H, et al. Genetic reconstruction of mouse spermatogonial stem cell self-renewal in vitro by Ras-cyclin D2 activation. *Cell Stem Cell*. 2009;5:76–86.
- [38] Lee J, Kanatsu-Shinohara M, Inoue K, et al. Akt mediates self-renewal division of mouse spermatogonial stem cells. *Development*. 2007;134:1853–1859.
- [39] Ma F, Zhou Z, Li N, et al. Lin28a promotes self-renewal and proliferation of dairy goat spermatogonial stem cells (SSCs) through regulation of mTOR and PI3K/AKT. *Sci Rep*. 2016;6:38805.
- [40] Wei Y, Cai S, Ma F, et al. Double sex and mab-3 related transcription factor 1 regulates differentiation and proliferation in dairy goat male germline stem cells. *J Cell Physiol*. 2018;233:2537–2548.
- [41] Wei X, Li K, Zhang G, et al. B7-H3 promoted proliferation of mouse spermatogonial stem cells via the PI3K signaling pathway. *Oncotarget*. 2018;9:1542–1552.
- [42] Huang YL, Huang GY, Lv J, et al. miR-100 promotes the proliferation of spermatogonial stem cells via regulating Stat3. *Mol Reprod Dev*. 2017;84:693–701.
- [43] Niu B, Wu J, Mu H, et al. miR-204 regulates the proliferation of dairy goat spermatogonial stem cells via targeting to Sirt1. *Rejuvenation Res*. 2016;19:120–130.
- [44] Mu H, Li N, Wu J, et al. PLZF-induced upregulation of CXCR4 promotes dairy goat male germline stem cell proliferation by targeting Mir146a. *J Cell Biochem*. 2016;117:844–852.
- [45] Spiller CM, Koopman P. Cell cycle control of germ cell differentiation. *Results Probl Cell Differ*. 2011;53:269–308.
- [46] Malumbres M, Barbacid M. Mammalian cyclin-dependent kinases. *Trends Biochem Sci*. 2005;30:630–641.

- [47] Dyson NJ. RB1: a prototype tumor suppressor and an enigma. *Genes Dev.* [2016](#);30:1492–1502.
- [48] Johnson J, Thijssen B, McDermott U, et al. Targeting the RB-E2F pathway in breast cancer. *Oncogene.* [2016](#);35:4829–4835.
- [49] Fruman DA, Chiu H, Hopkins BD, et al. The PI3K pathway in human disease. *Cell.* [2017](#);170:605–635.
- [50] Gonzalez E, McGraw TE. The Akt kinases: isoform specificity in metabolism and cancer. *Cell Cycle.* [2009](#);8:2502–2508.
- [51] Sanidas I, Polytarchou C, Hatziapostolou M, et al. Phosphoproteomics screen reveals akt isoform-specific signals linking RNA processing to lung cancer. *Mol Cell.* [2014](#);53:577–590.
- [52] Feng LX, Ravindranath N, Dym M. Stem cell factor/c-kit up-regulates cyclin D3 and promotes cell cycle progression via the phosphoinositide 3-kinase/p70 S6 kinase pathway in spermatogonia. *J Biol Chem.* [2000](#);275:25572–25576.
- [53] Liu T, Chen X, Li T, et al. Histone methyltransferase SETDB1 maintains survival of mouse spermatogonial stem/progenitor cells via PTEN/AKT/FOXO1 pathway. *Biochim Biophys Acta Gene Regul Mech.* [2017](#);1860:1094–1102.